Liquid Crystals
Publication details, including instructions for authors and subscription information:
http://www.informaworld.com/smpp/title~content=t713926090

Thermotropic ionic liquid crystals of pyridinium octylphosphate A N.M.R. and X-ray study

C. Chachaty[a]; T. Bredel[a]; A. M. Tistchenko[a]; J. -P. Caniparoli[a]; B. Gallot[b]
[a] CEA-IRDI, Département de Physico-Chimie, Gif-sur-Yvette cedex, France [b] Centre de Biophysique Moléculaire, Orleans cedex, France

To cite this Article Chachaty, C. , Bredel, T. , Tistchenko, A. M. , Caniparoli, J. -P. and Gallot, B.(1988) 'Thermotropic ionic liquid crystals of pyridinium octylphosphate A N.M.R. and X-ray study', Liquid Crystals, 3: 6, 815 — 824
To link to this Article: DOI: 10.1080/02678298808086538
URL: http://dx.doi.org/10.1080/02678298808086538

LIQUID CRYSTALS, 1988, VOL. 3, NOS. 6 AND 7, 815–824

Thermotropic ionic liquid crystals of pyridinium octylphosphate
A N.M.R. and X-ray study

by C. CHACHATY, T. BREDEL, A. M. TISTCHENKO and J.-P. CANIPAROLI

CEA-IRDI, Département de Physico-Chimie, DPC/BP 121, CEN de Saclay, 91191 Gif-sur-Yvette cedex, France

and B. GALLOT

Centre de Biophysique Moléculaire, 1 A, Avenue de la Recherche Scientifique, 47071 Orléans cedex, France

A thermotropic ionic lamellar phase from non-stoichiometric pyridinium octylphosphates has been investigated by multinuclear N.M.R. and X-ray diffraction. At room temperature and above, this phase is formed for pyridine to octylphosphoric acid molar ratios from 0·2 to 0·8. ^{2}H and ^{13}C relaxation experiments show that the pyridinium ion undergoes a very anisotropic motion with $D_{zz} > D_{xx} \gg D_{yy}$, z and x being the perpendicular direction to the ring and the c_2 symmetry axis, respectively. The order parameters given by the ^{2}H quadrupolar splittings and the ^{13}C chemical shift anisotropy (CSA) are $S_{zz} = 0{\cdot}13$, $S_{yy} = -0{\cdot}08$ and $S_{xx} = -0{\cdot}05$, showing that the pyridinium ring is preferentially oriented parallel to the lamellar plane. The ^{31}P CSA and the Cl–P dipolar splitting yield $S_{zz} = 0{\cdot}33$ and $S_{xx} \simeq S_{yy}$ for the octylphosphate anion. The order parameters of alkyl C–H bonds have been obtained from the J resolved two-dimensional ^{13}C N.M.R. spectra of oriented samples. Two limiting conformational models have been considered to calculate the S_{CH}. One of them is reasonably consistent with the structure derived from X-ray experiments and has been used to calculate the dipolar ^{31}P relaxation. Taking into account the CSA contribution, the relaxation measurements performed at 36, 121 and 202 MHz show that the octylphosphate anion undergoes a quasi-axial reorientation about the long molecular axis x with $D_{\parallel}/D_{\perp} = 4$ and $D_{\perp} \simeq 10^7$ rad/s at 300 K.

1. Introduction

In aqueous solutions, the alkaline salts of alkylphosphates present some unusual properties with respect to most known surfactants. They form micellar solutions and lyotropic liquid crystals for alkyl chains as short as C4 [1] and behave as very efficient complexants towards divalent transition ions. This latter property is dramatically enhanced upon micellization [2].

Beyond eight carbons, the solubility of sodium and potassium alkylphosphate decreases rapidly with the chain length while the minimum temperature of micellization (Krafft point) increases well above room temperature.

Experiments in progress in our laboratory show that these properties which restrict the potential applications of alkylphosphates as surfactants and complexants may be overcome by replacing the alkali cations by an organic cation-like pyridinium. Moreover, even in the absence of water, the pyridinium alkylphosphates give rise to liquid-crystalline phases of comparatively low melting points. The properties of

micellar solutions as studied by N.M.R. will be reported in a forthcoming paper [3]. The corresponding lyotropic mesophases are still under investigation. Here we report the main points of a resonance and relaxation study on the molecular orientation and dynamical behaviour in thermotropic liquid crystals from non-stoichiometric mixtures of pyridine (PYR) and octylphosphoric acid (OPA).

2. Experimental conditions

The octylphosphoric acid has been prepared by reaction of *n*-octyl alcohol on phosphorus oxychloride. The octylphosphoryl dichloride is hydrolized by a sodium hydroxide solution at pH 10. This solution is then acidified and the octylphosphoric acid is extracted by ether. The perdeuterated pyridine (isotopic purity > 99 per cent) was provided by the Service des Molécules Marquées at Saclay. The ^{2}H, ^{31}P and ^{13}C N.M.R. experiments were performed with Varian XL 100 (B_0 = 2·35 T), Bruker WH 90 (B_0 = 2·15 T), MSL 300 (B_0 = 7·05 T) and WM 500 (B_0 = 11·75 T) spectrometers.

The X-ray diffraction experiments were performed using a Guinier-type chamber. The system was maintained under high vacuum, the samples being contained between mylar windows in an aluminium cell. A bent quartz monochromator was used to focus the 1·54 Å copper radiation along a vertical line. The temperature was controlled to within $\pm 0{\cdot}5°$.

3. Results and discussion

The phase diagram represented in figure 1 has been delineated by N.M.R. spectroscopy, the liquid-crystalline nature of the samples being verified by observation under polarized light. At room temperature and above, a liquid-crystalline phase is formed for [PYR]/[OPA] molar ratios between 0·2 and 0·8. In this range, the phosphorus chemical shift anisotropy is found between − 13 and − 15 p.p.m. On cooling down the samples from the isotropic phase, the ^{2}H and ^{31}P N.M.R. show that the director becomes oriented perpendicular to the magnetic field.

Under our experimental conditions, only the first-order line of the X-ray diagram is observed. Upon water addition, the second-order line appears, whose position is characteristic of a lamellar phase. It is observed that the position of the first-order line depends linearly on the water weight fraction between 0 and 20 per cent so that it may be concluded that the anhydrous phase under study is also lamellar. For a [PYR]/[OPA] molecular ratio of 0·7, the total spacement of the layers is 26·5 Å. Calculating the density of the components from the molecular volumes given in [4], and using the method reported in [5], the thicknesses of the polar and non-polar layers are found to be 9·9 and 16·6 Å, respectively, with an area per polar head of 29 Å^2. Most of the N.M.R. experiments reported below have been done for this composition, which gives well-oriented samples.

The order parameters of the pyridinium cation have been obtained from the least square fit of the deuteron quadrupolar splittings (figure 2), by means of the expressions

$$\left.\begin{aligned}
\Delta\nu_{1,5} &= \tfrac{3}{4}\chi_o\left\{S_{xx} - \cos^2\phi_1[S_{xx} - S_{yy}] + \frac{\eta}{3}[2S_{yy} + S_{xx} + \cos^2\phi_1[S_{xx} - S_{yy}]]\right\},\\
\Delta\nu_{2,4} &= \tfrac{3}{4}\chi_m\left\{S_{xx} - \cos^2\phi_2[S_{xx} - S_{yy}] + \frac{\eta}{3}[2S_{yy} + S_{xx} + \cos^2\phi_2[S_{xx} - S_{yy}]]\right\},\\
\Delta\nu_{3} &= \tfrac{3}{4}\chi_p\left\{S_{xx} + \frac{\eta}{3}[2S_{yy} + S_{xx}]\right\},
\end{aligned}\right\} \quad (1)$$

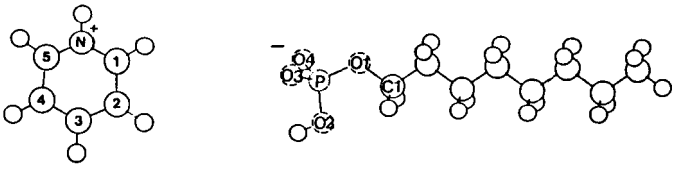

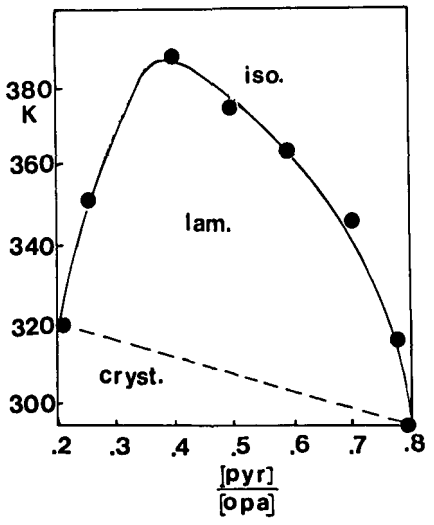

Figure 1. Phase diagram of the thermotropic ionic liquid crystals as a function of the pyridine to octylphosphoric acid molecular ratio.

where $\chi_{o,m,p}$ denote the quadrupolar coupling constants and η the asymmetry parameter of the electric field gradient tensor whose quasi-symmetry axis is the C–H bond. These parameters as well as ϕ, the angles defining the orientation of these bonds, are taken from [6]. The 8 kHz splitting clearly corresponds to deuteron 3; the assignment of the other ones is based on the least square fit of experimental data and confirmed by the C–H dipolar splittings given by two-dimensional N.M.R.: $\Delta\nu_{1,5} = 1450$ Hz, $\Delta\nu_{2,4} = 1490$ Hz and $\Delta\nu_3 = 1400$ Hz. The signs of the order parameters given in table 1 are deduced from the carbon 13 CSA: +18, +21 and +25 p.p.m. for carbons 1, 2 and 3, respectively. The exact principal values of the ^{13}C shielding tensor are unknown in the present case and most probably position-dependent. It is known, however, that for aromatic carbons, the largest principal value is in the +100, +120 p.p.m. range and corresponds to the perpendicular to the ring (see for instance [7]).

It is seen in table 1 that the order parameters of the pyridinium are approximately +0·13 perpendicular to the ring, −0·05 along the c_2 symmetry axis and −0·08 along the third direction. The pyridinium ring tends therefore to reorient perpendicular to the director of the mesophase. This trend may be understood considering the small spacing available between the polar heads of two adjacent layers (*ca.* 4 Å). The asymmetry of the ordering tensor, of the order of 0·2, indicates that the pyridinium reorientation is not axial. This is well confirmed by the ^2H and ^{13}C relaxation experiments (table 2) showing that the rotational diffusion tensor is strongly asymmetric, the fastest motion occurring about the direction perpendicular to the ring. The

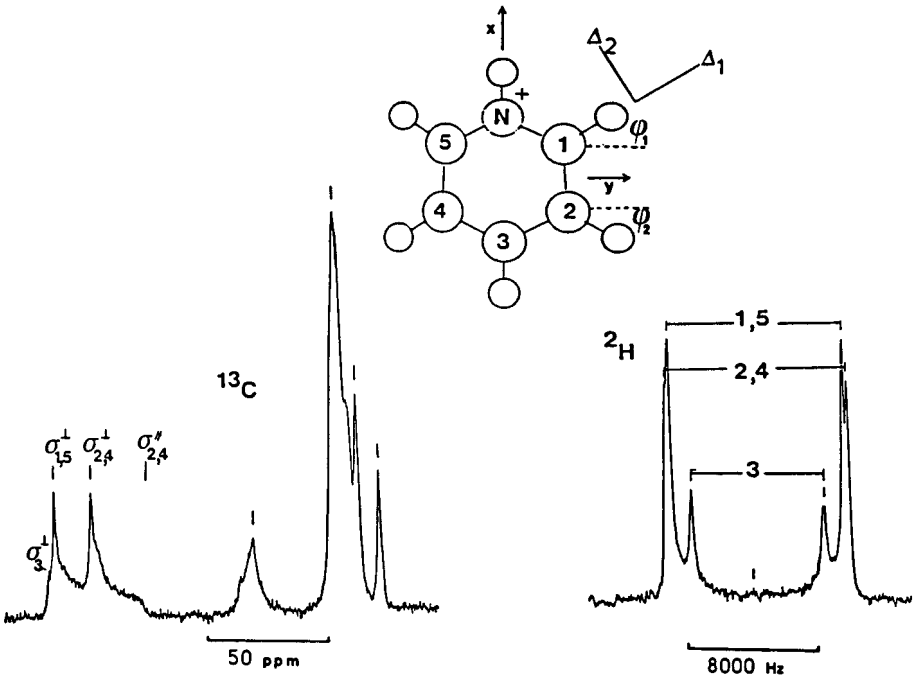

Figure 2. Carbon 13 and deuteron spectra for a [PYR]/[OPA] = 0·7 molar ratio. The deuteron spectrum corresponds to an oriented sample. Δ_1 and Δ_2 are two of the principal directions of the ^{13}C chemical shielding tensor.

Table 1. Pyridinium order parameters.

T/K	Deuteron number	Observed splittings kHz	Order parameters	Calculated splittings kHz†
	2, 4	10·888	$S_{xx} = -0.0559$	10·770
320	1, 5	10·497	$S_{yy} = -0.0805$	10·620
	3	8·276	$S_{zz} = +0.1364$	8·268
	2, 4	10·936	$S_{xx} = -0.0540$	10·820
315	1, 5	10·522	$S_{yy} = -0.0816$	10·650
	3	8·007	$S_{zz} = +0.1356$	7·999
	2, 4	10·937	$S_{xx} = -0.0540$	10·830
310	1, 5	10·546	$S_{yy} = -0.0817$	10·660
	3	8·007	$S_{zz} = +0.1358$	8·000
	2, 4	10·937	$S_{xx} = -0.0535$	10·820
305	1, 5	10·522	$S_{yy} = -0.0818$	10·640
	3	7·934	$S_{zz} = +0.1353$	7·926
	2, 4	10·717	$S_{xx} = -0.0494$	10·580
300	1, 5	10·229	$S_{yy} = -0.0810$	10·380
	3	7·349	$S_{zz} = +0.1304$	7·340

† With $\eta = 0.046$ and $\chi_p = 185$ kHz, $\phi_3 = 90°$; $\chi_0 = 184$ kHz, $\phi_1 = 31°{\cdot}7$; $\chi_m = 187$ kHz, $\phi_2 = -27°$.

diffusion coefficients have been obtained from the fit of the experimental relaxation rates, using the theory of Woessner for the reorientation of an ellipsoid in an isotropic liquid [8]. We have verified on the axial case that for such small order parameters, this theory is valid within the limits of experimental errors ($\pm$ 5 per cent). The discrepancies

Table 2. Determination of pyridinium rotational diffusion coefficients by ^2H and ^{13}C relaxations.

T/K	D_{yy} /(rad/s)	D_{xx} /(rad/s)	D_{zz} /(rad/s)	T_1/s Experimental	T_1/s Calculated	Positions
			^2H, 46 MHz			
				0·00708	0·0071	1, 5
300	10^6	$2·8 \times 10^8$	$2·3 \times 10^9$	0·00738	0·00703	2, 4
				0·00624	0·0059	3
				0·00801	0·00818	1, 5
305	10^6	$3·4 \times 10^8$	3×10^9	0·00802	0·00805	2, 4
				0·00662	0·00681	3
				0·01027	0·09944	1, 5
310	10^6	$4·4 \times 10^8$	4×10^9	0·01104	0·09789	2, 4
				0·00777	0·00826	3
				0·01453	0·01416	1, 5
320	10^6	$6·6 \times 10^8$	$6·5 \times 10^9$	0·01453	0·01393	2, 4
				0·01046	0·01184	3
			^{13}C, 75 MHz			
				0·2415	0·2313	1, 5
300	10^6	$1·6 \times 10^8$	$1·8 \times 10^9$	0·2473	0·2473	2, 4
				0·2562	0·2490	3
				0·231	0·254	1, 5
310	10^6	$2·4 \times 10^8$	$2·4 \times 10^9$	0·306	0·285	2, 4
				0·310	0·283	3
320	10^6	$3·8 \times 10^8$	$4·3 \times 10^9$	0·3707	0·3653	2, 4
				0·3618	0·3694	3

between the ^2H and ^{13}C data result possibly because the ^{13}C CSA has not been taken into a account in the calculation of relaxation rates.

The orientation and dynamical behaviour of the octylphosphate anion has been derived from the ^{31}P and ^{13}C N.M.R. and relaxation. The molecular orientation has been deduced from the P–Cl dipolar coupling of 220 Hz (figure 4) and from the phosphorus CSA of -15 p.p.m. (figure 3). The ^{31}P shielding tensor has been taken from the work of Kohler and Klein on monophosphates of biological significance [9]. This tensor is most likely averaged by rotation of the phosphate group about the P–O1 bond and/or by proton exchange among the oxygens, while the P–Cl dipolar coupling is only averaged by the molecular reorientation. Assuming an axially symmetric ordering tensor, the long molecular axis denoted as Δ_M is found to make an angle of 30° with the P–O1 bond with a molecular order parameter $S_z = \bar{P}_2(\cos\beta) = 0·33$. This axis coincides by less than 10° with the long axis of the effective inertial tensor, calculated as an average over all the accessible molecular conformers. This calculation shows in particular that the equivalent ellipsoid is nearly axially symmetric with an asymmetry parameter of 0·06, justifying our assumption about the ordering tensor.

The perdeuterated octylphosphate not being available, the order parameters of the C–H bonds have been determined by means of the *J*-resolved two-dimensional N.M.R. carbon 13 spectra with gated decoupling (figure 4). Using well-oriented samples, all the C–H dipolar couplings are resolved with the exception of carbons 4 and 5. Assuming that the segmental motions of the alkyl chain are much faster that the reorientational motion, the order parameters of the C–H bonds have been interpreted in terms of molecular conformations using computational procedures

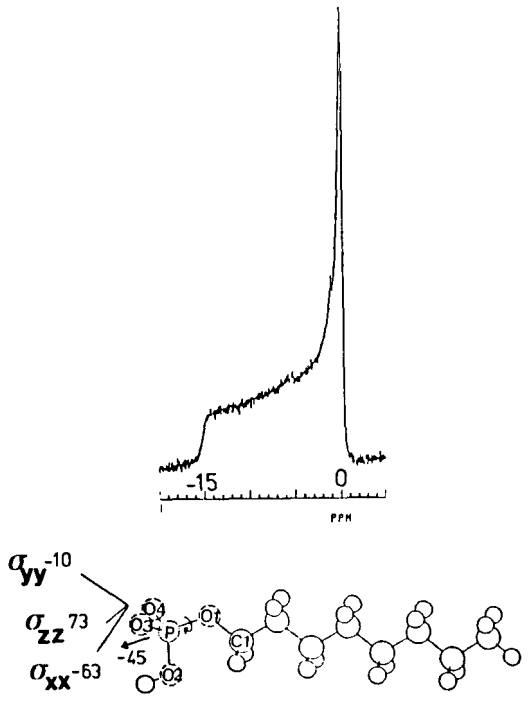

Figure 3. ^{31}P spectrum of a randomly oriented sample at 121·7 MHz. x, y and z denote the principal axes of the phosphorus shielding tensor before averaging by rotation about the O1–P bond.

described in [10] and [11]. For $S_{XX} = S_{YY}$, the ^{13}C–^{1}H dipolar splittings are given by the expression

$$\Delta\nu_{CH} = -\frac{\gamma_C\gamma_H h}{4\pi^2}(3\cos^2\theta - 1)r_{CH}^{-3}S_{CH}, \tag{2}$$

where

$$S_{CH} = \tfrac{1}{2}\langle 3l_{zZ}^2 - 1\rangle S_{ZZ}, \tag{3}$$

θ being the angle between the director and the magnetic field (90°), r_{CH} the carbon-to-proton distance, taken as 1·1 Å, and l_{zZ} the direction cosine of the C–H bond with respect to the Δ_M axis. The expression within brackets is a weighted average among all accessible conformers resulting from the trans-gauche isomerization of the oxyalkyl chain.

Two methods have been used to fit the C–H dipolar splitting removing the sterically hindered G^+G^- local forms from the calculations:

(*a*) the populations of the trans conformers about the O–C and C–C bonds are adjusted empirically, without explicit sterical constraints;

(*b*) as for (*a*), but the oxyalkyl chain is confined in a cylinder of 30 Å^2 section.

These two methods give nearly the same results (table 3). In method (*a*) there is a large predominance of the trans rotamers, the population of the fully extended structure representing 38 per cent of the 297 possible conformers. On the other hand, in method (*b*) the populations of the trans conformers approach those of a free

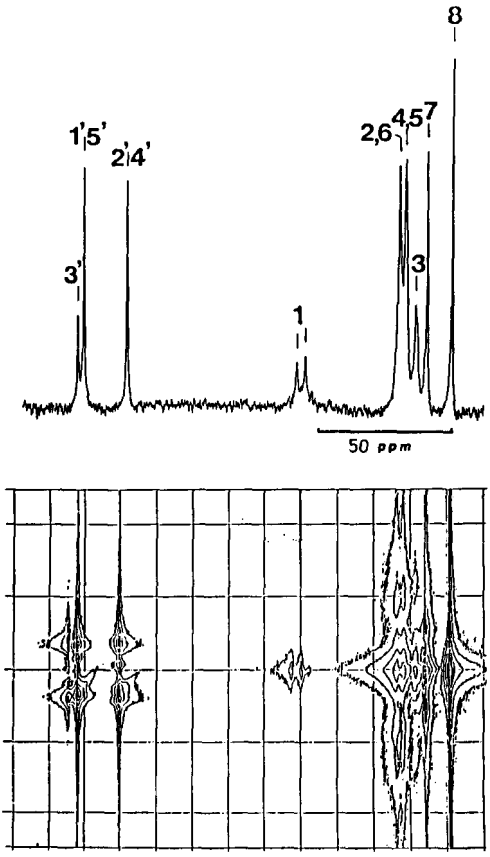

Figure 4. Top, ^{13}C spectrum of an oriented sample at 75·5 MHz; bottom, J resolved two-dimensional spectrum of the same sample. The C–H dipolar couplings have been determined on sections parallel to the J axis.

hydrocarbon (0·5–0·6) but the number of conformers is reduced to 37, with an enhanced contribution of G^+TG^- local forms (kinks).

The main difference between these two models is that there is no possibility of folding back the chain in model (*b*), whereas in model (*a*) the probability of finding a terminal methylene or methyl group at the vicinity of the interface with the polar layer is not negligibly small and could be evidenced by paramagnetic relaxation experiments [12]. The ^{31}P and ^{13}C relaxation experiments reported here do not allow such a discrimination; however the probability distribution of carbon distances to the polar layer may be computed from the S_{CH} order parameter, giving access to the density profile across the non-polar layer. Knowing the area per polar head and the thickness of this layer given above, both models yield a mean density of 0·78 g/ml, nearly that of a liquid hydrocarbon. However, the r.m.s. deviation about this mean value is 0·05 and 0·11 g/ml for models (*a*) and (*b*), respectively. These deviations which reflect the imperfections of the models are however in favour of model (*a*) (figure 5).

The determination of conformer populations is useful in the interpretation of the ^{31}P relaxation in term of molecular reorientation since providing the dipolar contribution. The other contribution is the CSA which becomes important at high magnetic field strengths. The T_1 measurements have been performed at 36, 121 and

Table 3. Octylphosphate order parameters $S_{zz} = 0{\cdot}33$, $S_{xx} \simeq S_{yy}$; ^{31}P chemical shift anisotropy $\Delta\sigma_{obs} = -15$ p.p.m., $\Delta\sigma_{calc} = -14{\cdot}1$ p.p.m.; ^{13}C–^{31}P dipolar slitting: $|\Delta\nu_{C-P}|_{obs} = 220$ Hz, $(\Delta\nu_{C-P})_{calc} = -248$ Hz.

	Oxyalkyl chain							
	O – C_1	– C_2	– C_3	– C_4	– C_5	– C_6	– C_7	– C_8
$P^{\dagger}_{trans}$	1	0·8	0·8	0·9	0·9	0·9	0·7	0·333
$P^{\ddagger}_{trans}$	1	0·5	0·5	0·45	0·45	0·45	0·4	0·333

	$\lvert\Delta\nu\rvert^{exp}_{CH}$/Hz	$\lvert S_{CH}\rvert_{exp}$	$\Delta\nu_{calc}$/Hz†	$\Delta\nu_{calc}$/Hz‡
1	3850	0·17	3742	3742
2	2970	0·13	3063	3027
3	2400	0·106	2413	2459
4	2100	0·093	2173	2499
5			1965	2192
6	1800	0·079	1776	1758
7	1150	0·051	1278	1320
8	300	0·013	291	—

† No confinement.

‡ Confined in a 30 Å^2 section cylinder.

† and ‡: the conformations containing G^+G^- local forms are removed so that the actual P_{trans} values are larger.

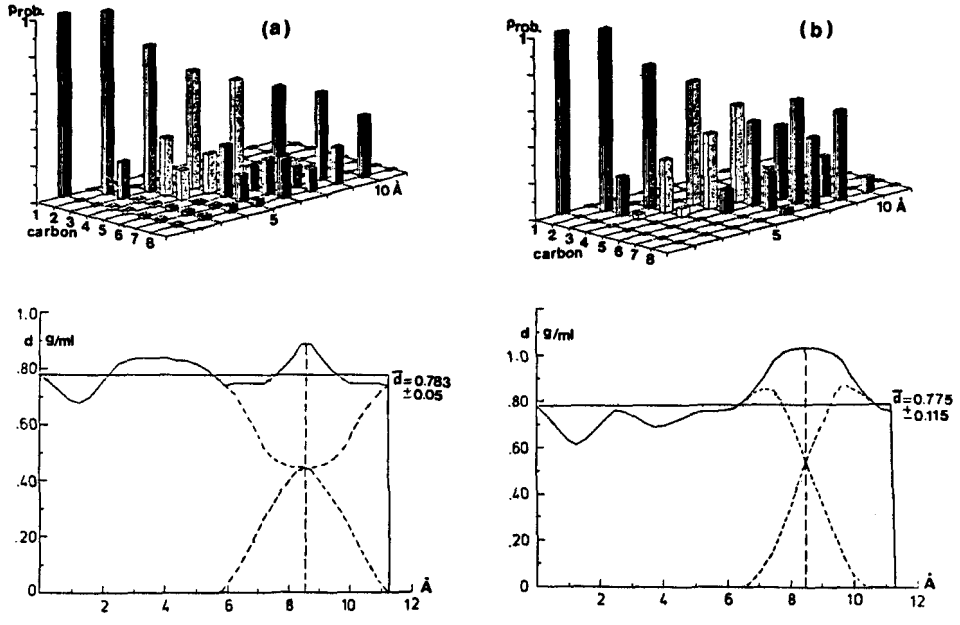

Figure 5. Computed density profile across the non-polar layer: (*a*) no explicit sterical constraints; (*b*) confinement in a 30 Å^2 section cylinder. The dotted lines correspond to the overlap of two hydrocarbon layers. The histograms represent the probabilities of carbon distances to the polar head, projected on the Δ_M axis.

202 MHz and interpreted by an anisotropic reorientation, using the expressions

$$(T_1^{-1})_{\text{dip}} = \tfrac{1}{2}(\gamma_I\gamma_S\hbar)^2 \sum_{-2}^{2} F_k^2[J_k^{(0)}(\omega_I - \omega_S) + 3J_k^{(1)}(\omega_I) + 6J_k^{(2)}(\omega_I + \omega_S)], \quad (4)$$

with

$$\left.\begin{aligned} F_0 &= \tfrac{1}{2}\langle(3\cos^2\phi - 1)r_{IS}^{-3}\rangle, \\ F_{\pm 1} &= \sqrt{\tfrac{3}{2}}\langle\sin\phi\cos\phi\, r_{IS}^{-3}\rangle, \\ F_{\pm 2} &= \sqrt{\tfrac{3}{8}}\langle\sin^2\phi\, r_{IS}^{-3}\rangle, \end{aligned}\right\} \quad (5)$$

$$(T_1^{-1})_{\text{CSA}} = \omega^2 \sum_{-2}^{2} F_k'^2 J_k^{(1)}(\omega_I) \quad (6)$$

with

$$F_k' = \sum_{k'=-2}^{2} D_{kk'}^{(2)} F_{k'}, \quad (7)$$

$D_{kk'}^{(2)}$ being the second-rank Wigner matrix, and

$$F_0 = \sqrt{\tfrac{2}{3}}(\sigma_{zz} - \tfrac{1}{2}(\sigma_{xx} + \sigma_{yy})), \quad F_{\pm 1} = 0, \quad F_{\pm 2} = \tfrac{1}{2}(\sigma_{xx} - \sigma_{yy}). \quad (8)$$

In expressions (4) and (6) the spectral densities are of the form

$$J_k^{(k')}(\omega) = [A_k^{(k')}\cos^4\theta + B_k^{(k')}\cos^2\theta + C_k^{(k')}]\tau_k/(1 + (\omega_{k'}\tau_k)^2), \quad (9)$$

the dependence of the A, B and C coefficients upon the second and fourth rank order parameters have been taken from [13]. For comparatively small values of $\bar{P}_2(\cos\beta)$, the reorientation correlation times are given by [14]

$$\tau_k = [6D_\perp + k^2(D_\parallel - D_\perp)]^{-1}. \quad (10)$$

The contribution of collective motions which introduces a $\omega^{-1/2}$ dependence of relaxation rates has been considered in our calculations, without improving the agreement with experiment. Furthermore, this contribution does not account for the angular dependence of the ^{31}P relaxation measured at 121 and 202 MHz on a randomly oriented sample. At room temperature the octylphosphate undergoes a slow anisotropic reorientation in the 10–20 ns time scale range (table 4). Raising the temperature to the melting point results in a continuous decrease of the ^{31}P spin-lattice relaxation time, even at 36 MHz. The rate of internal motions have been estimated from the ^{13}C T_1 relaxation times at 22 and 75 MHz, using spectral densities of the form

$$J(\omega) = S_{CH}^2 \frac{\tau_s}{1 + \omega^2\tau_s^2} + (1 - S_{CH}^2)\tau_f. \quad (11)$$

This corresponds to the model-free approach of Lipari and Szabo [15] which may be extended to liquid crystals under some conditions discussed in [16]. Here τ_s has been taken as equal to the reorientation correlation time τ_0 of the Δ_M axis. The fast correlation times τ_f which correspond to the torsional and rotational motions along the chain have been derived from the least square adjustment of the ^{13}C relaxation times (table 4). They are at least two orders of magnitude shorter than τ_0, justifying our calculations of conformer populations from the order parameters of C–H bonds.

Table 4. Octylphosphate ^{31}P and ^{13}C relaxation times at 300 K.

^{31}P†

		B_0/T		
		2·15	7·05	11·75
T_1	exp (*s*)	0·63	1·80	2·0
T_1	calc	0·41	1·56	2·1

^{13}C‡

		B_0/T		
	T_1/s	2·35	7·05	τ_f/ps
C_1	exp	0·21	0·324	90
	calc	0·21	0·265	
C_3	exp	0·37	0·390	60
	calc	0·35	0·390	
$C_{4,5}$	exp	0·39	0·500	50
	calc	0·41	0·465	
C_7	exp	0·70	1·000	30
	calc	0·73	0·774	
C_8	exp	1·9	2·300	8
	calc	1·9	1·940	

† Computed with $\tau_0 = 1{\cdot}5 \times 10^{-8}$ s, $D_\parallel/D_\perp = 4$ (equations (4) and (6)).

‡ Computed by means of equation (11), with $\tau_s = 1{\cdot}5 \times 10^{-8}$ s taking the S_{CH} values of table 3.

References

[1] Perly, B., Quaegebeur, J. P., Chachaty, C., and Gallot, B., 1985, *Molec. Crystals liq. Crystals*, **128**, 287.

[2] Chevalier, Y., and Chachaty, C., 1985, *J. Am. chem. Soc.*, **107**, 1102.

[3] Chachaty, C., Ahlnäs, T., Lindström, B., Nery, H., and Tistchenko, A. M., 1988, *J. Coll. Interface Sci.* (in the press).

[4] Millero, F. J., 1971, *Chem. Rev.*, **71**, 147.

[5] Gallot, B., 1978, *Adv. Polym. Sci.*, **29**, 85.

[6] Jacobsen, J. P., and Jonas Pedersen, E., 1981, *J. magn. Res.*, **44**, 101.

[7] Mehring, M., 1982, *The Principles of High Resolution NMR in Solids* (Springer Verlag).

[8] Woessner, D. E., 1962, *J. chem. Phys.*, **37**, 647.

[9] Kohler, S. J., and Klein, M. P., 1976, *Biochemistry*, **15**, 967.

[10] Chachaty, C., and Langlet, G., 1985, *J. Chim. phys.*, **82**, 613.

[11] Chachaty, C., Quaegebeur, J. P., Caniparoli, J. P., and Korb, J. P., 1986, *J. phys. Chem.*, **90**, 1115.

[12] Chachaty, C., and Korb, J. P., 1988, *J. phys. Chem.* (in the press).

[13] Freed, J. H., 1977, *J. chem. Phys.*, **66**, 4183.

[14] Nordio, P. L., and Segre, U., 1978, *The Molecular Physics of Liquid Crystals*, edited by G. R. Luckhurst and G. M. Gray (Academic Press), p. 407.

[15] Lipari, G., and Szabo, A., 1982, *J. Am. chem. Soc.*, **104**, 4546.

[16] Brown, M. F., 1984, *J. chem. Phys.*, **80**, 2833.